Condition Assessment of Reinforced Concrete Systems with Fusion-Bonded Epoxy-Coated Rebars

Deepak K. Kamde,‡ Sylvia Kessler,** and Radhakrishna G. Pillai****

Corrosion assessment of reinforced concrete (RC) structures with fusion-bonded-epoxy (FBE)-coated steel rebars is a challenge because the common inspection methods and data cannot be applied or interpreted in the same way as that for the systems with uncoated rebars. If corrosion detection tools based on techniques such as half-cell potential (HCP), linear polarization resistance (LPR), or electrochemical impedance spectroscopy (EIS) are used for the assessment of systems with FBE-coated steel rebars without considering the difference in the electrochemical conditions between coated and uncoated systems, then the interpretation can result in the inability to detect ongoing corrosion. Therefore, the objective of this paper is to examine the suitability of these inspection methods and data to be applied to the RC systems with FBE-coated steel rebars. For this, the suitability of test methods on HCP, LPR, and EIS for assessing corrosion conditions of RC structures was assessed using laboratory specimens and field structures. Field investigation using HCP shows that the HCP could not detect corrosion of FBE rebars unless the coating was severely disbonded due to corrosion of steel rebars. Also, the suitability of test methods based on HCP, LPR, and EIS was assessed by additional laboratory specimens. Although complex, only the EIS technique could reliably detect the corrosion conditions of the FBE-coated steel rebars embedded in concrete. Therefore, a way forward to assess RC structures using the EIS technique is proposed.

KEYWORDS: bridge, building, coating, concrete, condition assessment, corrosion, epoxy, steel

INTRODUCTION

The motivation to use fusion-bonded-epoxy (FBE)-coated steel rebars in concrete structures is to prevent or delay the initiation of corrosion of steel rebars. However, a lot of literature reports that reinforced concrete (RC) structures with FBE-coated steel rebars can exhibit corrosion within a few decades of service, especially in a chloride-laden environment.[1-2] For instance, Florida has a stock of approximately 300 RC bridges with FBE-coated steel rebars in the marine environment. Some of these bridges have experienced corrosion within two decades after construction.[1] Similarly, numerous RC structures with FBE-coated steel rebars might already be experiencing corrosion that is probably yet to be noticed. In such cases, corrosion can propagate under the film and may not be visible until it is too late.[3] FBE-coated steel rebars with damage/degraded coating undergo localized corrosion, which may lead to significant loss of structural capacity.[4] Hence, there is a need to assess the effectiveness of the epoxy coating on steel rebars in controlling corrosion. The first step to control corrosion is to know the corrosion condition of steel rebars in concrete using electrochemical inspection techniques. A lot of literature reports the strategies to assess the condition of RC structures with uncoated steel rebars, namely (a) updating the probabilistic residual service life estimates of RC structures or (b) by periodic inspections using electrochemical tests, such as measurement of half-cell potential (HCP) mapping,[5-7] measuring the rate of corrosion etc.[8-10] Many of these references propose guidelines and recommendations to do condition assessment of RC structures with uncoated steel rebars. However, the condition assessment of RC structures with FBE-coated steel rebar can be challenging due to the high resistance of good-quality FBE coatings and unknown locations of defects and associated changes in the electrochemical behavior. Therefore, the strategy for condition assessment of RC structures with uncoated steel rebars cannot be directly implemented to assess the structures with FBE-coated steel. This paper investigates the capability of test methods based on HCP, linear polarization resistance (LPR), or electrochemical impedance spectroscopy (EIS) in assessing the RC systems with FBE coated steel rebars in the lab and field. Results from this paper show that the existing test methods used for RC systems with uncoated steel rebars may not be suitable to assess the corrosion condition of RC systems with FBE coated steel rebars. Also, this paper provides directions toward developing a suitable electrochemical method to assess the corrosion condition of RC systems with FBE-coated steel rebars.

1.1 | Corrosion of Fusion-Bonded Epoxy-Coated Rebars

The function of FBE coating is to serve as a barrier for the electronic and ionic movements between the steel and concrete and along the steel/concrete interface—to delay the initiation of corrosion. The electrical resistivity of a good-quality FBE coating is significantly high (>10^6 Ω·cm).[11-13] Generally, FBE-

Submitted for publication: January 17, 2021. Revised and accepted: October 25, 2021. Preprint available online: October 25, 2021, https://doi.org/10.5006/3786.
‡ Corresponding author. E-mail: deepak.kamde89@gmail.com.
* Postdoctoral Researcher, Department of Civil Engineering, Indian Institute of Technology Madras, Chennai, India.
** Chair of Engineering Materials and Building Preservation, Helmut-Schmidt-University/University of the Federal Armed Forces Hamburg, Hamburg, Germany.
*** Associate Professor, Department of Civil Engineering, Indian Institute of Technology Madras, Chennai, India.

AQ1

ISSN 0010-9312 (print), 1938-159X (online)

coated steel rebars initiate corrosion when a sufficient amount of chloride ions penetrate through the concrete and coating and reach the steel rebar (beneath the coating).[14-15] But, possible defects (say, scratches, cracks, peeling off, etc.) in the coating due to the inadequate production, transportation, handling, and installation processes can adversely affect the barrier function[1,16-19]—leading to localized corrosion. The challenge of corrosion assessment of such systems is to identify the locations of corrosion (mostly localized) of steel rebars. In systems with FBE-coated steel rebars, the information of possible flaws or defects in the coating is important because corrosion initiation can take place extensively at those locations. Even though steel corrosion initiates at a flaw, the resulting rate of corrosion is limited due to restricted polarizable steel surface area.[8] Ideally, only steel at the flaws (cracks, scratch, etc.) on the same rebar can serve as anode and cathode because they need to be connected electrically. However, in many structures (e.g., many structures in the Florida Keys), an appreciable degree of interconnectivity has been observed between FBE-coated steel rebars due to unintended damage, such as scratches, cracks, etc., in FBE coating at the intersections of the rebars. Also, the polarizable area can increase over time due to the cathodic and anodic disbondment of the coating.[18] In ideal cases without damage to the coating, the microcells and macrocells can form on the same rebar (i.e., cathodes and anodes exist on the same rebar).[20] Therefore, the high electrical resistance of the coating can complicate common corrosion condition assessment methods used for uncoated steels. The suitability of test methods based on these techniques is discussed next.

1.2 | Half-Cell Potential Measurements

HCP measurement is a common technique used to assess the probability of corrosion of steel in RC systems.[21-24] This is based on the principle that actively corroding areas on steel can show a more negative electrical potential than the passive areas on steel. The resulting potential field is detectable with a voltmeter by measuring the potential difference between the rebar in concrete (via an electrical connection) and a reference electrode, which is attached electrolytically to the concrete surface. HCPs of embedded steel rebars are measured at various points (say, grid points) on the concrete surface. The locations with more negative potentials than the adjacent points and combined with pronounced potential gradients are indicators of the high probability of corrosion. However, HCPs provide only the information about the probability of corrosion during the measurement and do not provide estimations on past or future corrosion conditions or the rate of corrosion. The interpretation of HCP data can be challenging in case of varying moisture conditions in the concrete and when the resistivity of concrete is high.[22,25-27] All these are well-reported for concrete with uncoated rebars. The following two are the main factors affecting the application of the HCP technique in RC systems with FBE-coated steel rebars. First, the significantly high resistance of FBE coating; and second, the restricted potential fields due to the FBE coating. Potential fields can develop only between the exposed steel portions at the flaws or cracks in the coatings. Nondestructively detecting the locations of flaws/cracks is another challenging task. Some references report that the EIS-based test methods could evaluate the coating condition of FBE coating in concrete structures.[3,28] However, assessing the condition of FBE coatings and FBE-coated steel rebars in large infrastructure systems such as bridges and buildings is not fully explored. Therefore, one objective of the current paper is to investigate the applicability of the HCP technique in detecting corrosion of FBE-coated steel rebars in concrete.

1.3 | Linear Polarization Resistance Measurements

LPR technique is widely used to assess corrosion in RC systems. During LPR measurements, the embedded rebar is polarized slightly by applying small voltage variations, typically less than ±20 mV, from its corrosion potential. The resistance to polarization is the ratio between the applied potential and the corresponding difference in measured current across the free corrosion potential. In other words, the corrosion current density can be obtained by dividing the Stern-Geary constant (B) by the R_p taken into account the polarized area.[9] Ideally, the polarized area is not the entire steel surface in contact with concrete, as current attenuation from the counter electrode causes nonuniform polarization in extended systems unless the area is restricted using a guard ring. Therefore, for simplicity, the nominal surface area of the steel rebar is considered, which is in contact with the concrete. Therefore, surface-normalized resistance to polarization (R_p) is calculated by multiplying the surface area of the working electrode to the resistance of polarization.[29] For FBE-coated steel rebars, the nominal surface area of steel is equal to the total area of the defects, which is not possible to measure in most cases. Because the area of the defects is unknown, the resulting corrosion rate measurements can only be indicative of the relative corrosion activity. Accurate quantification of the rate of corrosion is not possible unless the area of damage is quantified. In addition, the LPR measurements give the bulk electrochemical response (i.e., a combined response) from solution, mortar, coating, steel/coating interface, etc. As the resistance of pristine FBE coating is significantly high, the combined response will be dominated by the resistance of the coating, which makes it difficult to extract the resistance to polarization of the steel/coating interface and monitor R_P to detect ongoing corrosion processes. Considering the high resistance of FBE coating, the LPR technique may be useful to detect corrosion if the coating is significantly damaged (say, when the polarizable area is large).[30-31] In a seven y study on FBE-coated rebars in chloride-contaminated concrete, the assessment of corrosion using LPR measurements was possible only because of the high corrosion rates of steel rebars in some specimens.[32] However, the ability of the LPR technique in assessing corrosion conditions for systems with FBE-coated steel rebars is not well reported in the literature, which is one of the foci of this paper.

1.4 | Electrochemical Impedance Spectroscopy Measurements

The EIS technique is based on the application of an alternating current (AC) signal of small amplitude (say, 1 to 10 mV) to the working electrode. The working electrode is the metal at which the electrochemical reactions of interest occur. Typically, materials with pure electrical resistance follow Ohm's law, i.e., R = V/I, where R is the resistance of the systems, V is the potential difference between the anode and cathode, and I is the magnitude of current between anode and cathode. However, the steel/concrete interface is not a purely resistive system. It consists of other circuit elements such as capacitor and inductor. For such systems, the impedance (Z) is the measure of the ability to prevent the electrochemical reactions in the system; and Z is measured by applying sinusoidal potential excitation and measuring the response as an AC signal. Unlike bulk response from LPR, the EIS provides the component response (i.e., from

each element) of the system being assessed.[33] Sagues and Zayed proposed one of the first methods based on EIS to calculate the corrosion rate of FBE-coated steel rebars in concrete with damaged coating.[34] However, adequate calculations on corrosion rates are possible only when the damaged area of the coating is known, which makes it difficult to apply in the field structures with embedded FBE-coated steel rebars. Lau proposed another test method based on the EIS technique to estimate the damaged surface area of the coating. In this, the ohmic resistance of the electrolyte was measured, which is assumed to be filling the defects or flaws in the coating. The measured ohmic resistance of the coating was reported to be inversely proportional to the area of defects.[28,35] These results are a first step toward applying EIS as a diagnostic technique to assess the performance of FBE-coated steel rebar and possible field applications. A few recent references suggest assessing RC systems with FBE-coated steel rebars using the EIS technique in laboratories.[14,28,36-43] The test methods developed for laboratory specimens may be modified for assessing such systems in RC structures. From the laboratory studies, it is clear that the corrosion condition of steel/coating interface responds to low frequencies (say, 1 Hz or less),[44] which can be assessed by monitoring the parameters, such as resistance to the polarization of steel/coating interface, $R_{P,\ S\text{-}C}$; Phase angle, θ; etc.

EXPERIMENTAL PROGRAM

The experimental program is divided into two phases. Phase 1 includes the field assessment of RC systems with FBE-coated steel rebars using the HCP technique, which was conducted with the support of the Department of Civil and Environmental Engineering at the University of South Florida, Tampa, Florida, USA, and Florida Department of Transportation. Phase 2 includes the laboratory studies using HCP, LPR, and EIS techniques in assessing corrosion of FBE-coated steel rebars. Phase 2 was conducted at the laboratories of the University of South Florida, Tampa, Florida, USA, and the Indian Institute of Technology Madras, Chennai, India.

2.1 | Phase 1: Field Assessment (Using Half-Cell Potential) of Fusion-Bonded-Epoxy-Coated Rebars

2.1.1 | Condition Assessment of Niles Channel Bridge

Figure 1(a) shows the location of the Niles Channel Bridge (built in 1982) between Ramrod Key and Summerland Key in the tropical zone of Florida. The bridge was built with FBE-coated steel rebars complying to ASTM 775 and placement guidelines valid during construction.[45] The guidelines allowed a maximum of 2% unrepaired coating damage. The Niles Channel Bridge was built with drilled shafts supporting columns with connecting struts. A majority of the columns had visible severe corrosion and large cracks on the concrete surface, spalled/delaminated concrete. Most of them were repaired with conventional patch repair and corrosion protection procedures with sacrificial sprayed-zinc anodes in 1996. Field investigation observed that some of the repair work had deteriorated. After the visual survey, Strut 12 (size: 0.9 m × 1.8 m; Figure 1[b]) was selected for further measurements because it was not repaired in previous maintenance. The lower part of the strut showed large cracks (with a width up to 2.6 mm), which appeared to be the only visually apparent deficiency. No concrete delamination was observed or detected by hammer sounding. There was no option to establish an electrical connection to the rebar, the HCP measurement has been studied with a second reference electrode placed at one corner being a reference point.[46] The grid size was 15 cm × 15 cm, and the concrete surface was prewetted at 20 min prior to the measurement according to the German specification.[24]

2.2 | Phase 2: Laboratory Assessment (Using Half-Cell Potential, Linear Polariztion Resistance, and Electrochemical Impedance Spectroscopy) of Fusion-Bonded-Epoxy-Coated Rebars

2.2.1 | Applicability of Half-Cell Potential Measurements on Fusion-Bonded-Epoxy-Coated Rebars

The specimens used for the laboratory investigation of HCP were part of a former project on the corrosion performance of FBE-coated rebar;[47] see Figures 2(a) and (b). Each specimen contains five FBEcoated rebars; Specimen 1—Rebars A to E and Specimen 2—Rebars F to J. A total of four coating defects were created on each rebar by cutting the coating with a sharp knife and peeling off small sections of the epoxy layer to reveal the metal substrate (see Figure 2[c]). The individual defect size is about 3 mm× 5 mm, which corresponds to a total defect area of 15 mm^2, which is ≈1% of the total surface area of the rebar. These defects were made on the coating surface facing the concrete surface used to measure the HCP. Additionally, titanium reference electrodes were installed close to each rebar, which

(a) (b)

FIGURE 1. *Niles Channel Bridge location and the investigated strut (0.9 m × 1.8 m). (a) Google map and (b) photograph of the strut.*

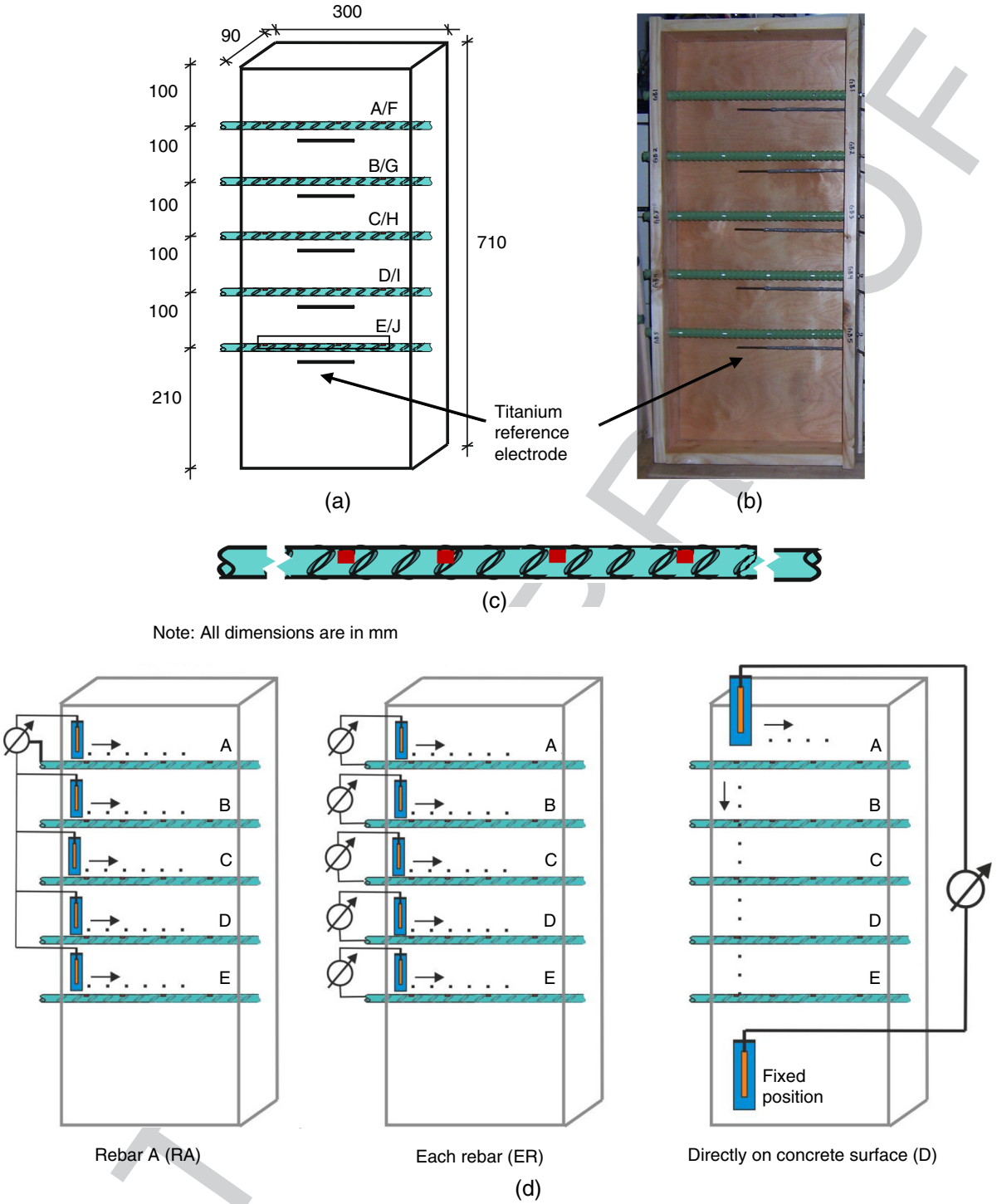

FIGURE 2. *Details of column specimens used for laboratory studies using HCP [Alphabets A to E and F to J indicate the rebar IDs in Specimens 1 and 2]. The surface area of cathode was taken as several times the surface area of nominal surface area of working electrode (i.e., coated steel rebar). (a) Schematic, (b) photograph, (c) closeup of rebar showing damage to coating, and (d) schematic showing the procedures to measure the HCPs.*

are calibrated against an external copper/copper-sulfate-electrode (CSE) before starting and at the end of each electrochemical measurement. The potential shift before and after each measurement was less than 2 mV. Considering the challenges associated with the measurement of HCP of FBE-coated steel rebars, the HCP measurements were recorded in three ways (see Figure 2[d]): (i) electrical connection with Rebar A and Rebar F, RA/RF; (ii) electrical connection to each rebar, ER; and (iii) without electrical connection to the rebar but with a fixed reference electrode as reference (D); see Figure 2(d). For Method D, one of the CSE was maintained at the constant reference position while the second CSE was moved along the concrete surface and used to measure the corrosion potentials of the isolated rebars. However, some FBE-coated steel rebars

may have an electrical connection between them due to damage or scratches to coating, if any, at the intersection of two rebars. In addition, such systems with damage will have reduced ionic resistance between adjacent rebars. To simulate this condition, the rebars were short-circuited externally with electrical wires, this condition is indicated as "sc".

The aim of the laboratory experiment is to study the detectability of ongoing corrosion at the flaws of FBE-coated rebar under controlled conditions. Therefore, after finishing the corrosion-free experiments, Specimen 2 was placed in 3% NaCl solution up to the level of the rebar "J". The rebars in Specimen 1 were polarized by impressed current technique to simulate ongoing corrosion. For this, the positive end of the DC power supply was connected to the Rebar E. A cathode (stainless steel mesh) with a several times larger surface area of the Rebar E was connected to the negative terminal of the DC power source without any resistor in between the rebars. A potential difference was applied between Rebar E and the cathode until an impressed corrosion current density was ≥ 0.5 μA/cm². The polarization potential for Rebar E was −240 mV_{CSE}. Then, to simulate the condition where one of the coated rebars is corroding and they are in physical contact with each other by highly resistive FBE coating, the adjacent rebars were interconnected with resistors of electrical resistance of 8.2 MΩ and 5.6 MΩ. Note that resistors with one electrical resistance were connected at a time. For example, first, all adjacent rebars were connected to each other by resistors with electrical resistance of 8.2 MΩ; then, the resistors were replaced with resistors of 5.6 MΩ. The electrical resistance of 8.2 MΩ and 5.6 MΩ were chosen as they are similar to the electrical resistance of typical FBE coating on rebars in structures.[48] Similar to the "sc" case for RC systems with "no corrosion," rebars were short-circuited to account for the effect of corrosion and damage to coating on various corrosion measurements, these conditions are indicated as "1 pol ER sc," "1 pol RA sc," and "1 pol D sc."

2.2.2 | Condition Assessment of Fusion-Bonded-EpoxyCoated Steel Rebar Using Linear Polarization Resistance and Electrochemical Impedance Spectroscopy

Figure 3(a) shows the schematic and photographs of lollipop-type specimens used to evaluate the suitability of LPR and EIS. Five lollipop specimens (total of 15) each with (i) uncoated steel, (ii) FBE-coated steel with no damage (FBEC-ND), and (iii) FBE-coated steel with scratch damage (FBEC-SD) were cast. For FBEC-SD specimens, controlled defects were created by scratching the coating on central seven to nine ribs of steel rebar using emery paper. The maximum total defect size was limited to 0.6% of the surface area of the steel rebars, which is less than the allowable damage level of 1%, as prescribed in ASTM A775-17.[49] Figures 3(a) and (b) show the procedure to prepare the lollipop specimens. For this, uncoated FBEC-ND and FBEC-SD steel rebars of 8 mm diameter were cut to 110 mm length. Then, one end of all of the steel was drilled with a 3.4 mm diameter hole (see Figure 3[a]), and a threaded stainless-steel rod was fastened to make the electrical connections required for the electrochemical tests. The uncoated steel pieces were cleaned and degreased using ethanol and ultrasonic cleaner, and FBE-coated steels were degreased using ethanol. Then, 5 mm long portion at the end of the steel rebars, the junction of FBE-coated steel rebar and stainless steel, and about 5 mm to threaded stainless steel, were covered with the heat-shrink tube. The gap, if any, between the threaded stainless-steel rod and heat-shrink tube was filled with low viscous epoxy to avoid the entry of moisture/chlorides (Figure 3[b]). The prepared steel pieces were placed in 110 mm long cylindrical molds (say, centrifuge tubes, with conical bottom) and centered by passing it through the hole at the center of the plastic cap. Mortar with water: binder: sand ratio of 0.5: 1: 2.75 was placed in molds to achieve a cover of about 10 mm. Then, the specimens were cured in plastic molds for one day in the laboratory environment (25±2°C and 65±5% relative humidity). After demolding, to allow only the center 50 mm portion of the specimen to be in direct contact with the immersion solution, the top and bottom portions of the specimens were coated with three layers of epoxy, as shown in Figure 3(c). Each layer of epoxy was cured for 2 h to 3 h, as per the manufacturer's guidelines. After curing of epoxy layers, the lollipop specimens were moved to the fog room (25±2°C and >95% relative humidity) for curing until 28 d. Then, the specimens were moved out of the curing room for chloride exposure and corrosion testing.

Figure 3(d) shows the photograph of the corrosion cell (three-electrode system) used for LPR and EIS tests. The embedded steel rebar was the working electrode. A nickel-chromium mesh of at least two times the surface of the nominal surface area of coated steel rebars was placed circumferentially to the lollipop specimen was the counter electrode, and a saturated calomel electrode (SCE) was the reference electrode. The simulated concrete pore solution (0.03% $Ca(OH)_2$ + 2.23% KOH + 1.04% NaOH + 96.6% of distilled water) contaminated with 3.5% NaCl was used as the immersion solution. The specimens were exposed to 2 d of wet followed by 5 d of a dry period. LPR and EIS tests were performed after every wet period.

For LPR measurements, the scan rate and scan range are two important input parameters, and their choices can alter the measured corrosion characteristics. The scan rate controls how fast the applied potential is scanned. The faster scan rates can lead to reduction in the size of the diffusion layer[50]—resulting in higher measured output currents. It is reported that the scan rate of 0.05 mV/s is sufficient to charge the capacitance of double layer in steel-cementitious systems with low resistivity (say, surface resistivity <21 kΩ·cm; OPC systems).[42] The scan rate greater than 0.05 mV/s can result in a decrease of calculated R_p due to the increase of disturbance in the double layer (i.e., charging current across the double layer). To avoid any disturbance, a scan rate of 0.05 mV/s would be suitable, as recommended by Ameer, et al., and Rengaraju, et al.[51-52] In the case of scan range, a value greater than $\pm 15 \times 10^{-3}$ V vs. open-circuit potential (V_{OCP}) can lead to a nonlinear response.[51] Therefore, the following testing parameters were used: scan range of±0.015 V with respect to the OCP at a scan rate of 0.05×10^{-3}V/s. The coated steel surface area within the exposed surface area of mortar (i.e., the surface area within 50 mm midlength, 12.6 cm^2) was considered as the surface area of the working electrode.

For the EIS measurements, AC potential amplitude of ±10 mV, frequency range from 10^6 Hz to 0.01 Hz, and DC potential maintained at OCP were used; and 10 data points per decade were collected. The coated steel surface area within the exposed surface area of mortar (i.e., the surface area within 50 mm midlength, 12.6 cm^2) was considered as the surface area of the working electrode. The total coated steel surface area was considered because the surface area of the defect (pinholes, cracks on coating, etc.) was not measured. Also, such measurements are not possible at the site. The signal response was analyzed, and resistances offered by each layer (denoted as $R_{p,\,M}$, $R_{p,\,C}$, and $R_{P,\,S\text{-}C}$ for mortar, coating, and steel/coating interface, respectively) were quantified using the proposed

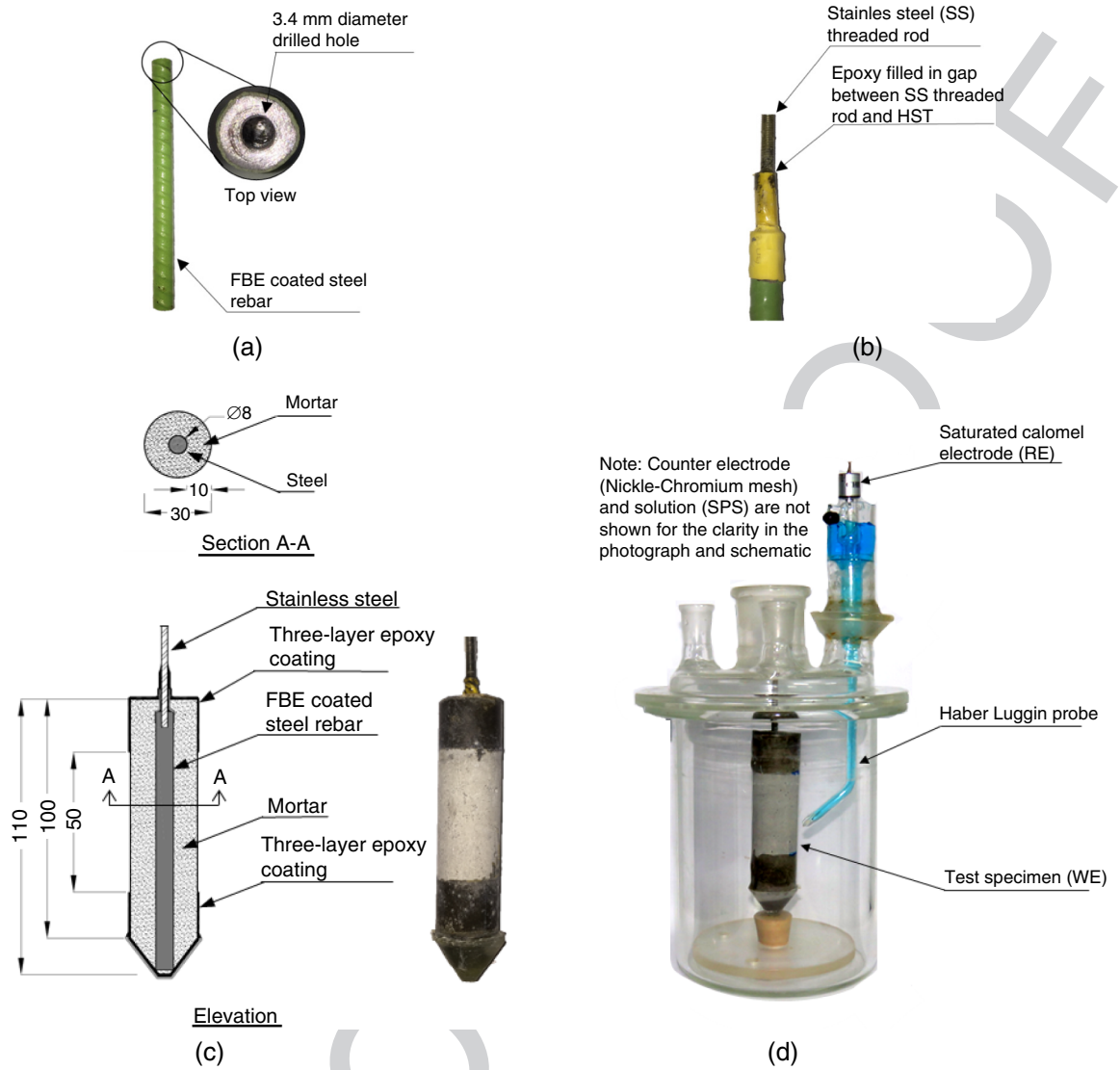

FIGURE 3. *Details of lollipop specimens used for laboratory studies using LPR and EIS. The surface area of a counter electrode was taken as several times the surface area of nominal surface area of a working electrode. (a) 110 mm long cut epoxy-coated steel rebar, (b) heat shrink tube applied at the end of FBE-coated steel rebar and epoxy filled in the gap between heat shrink tube and stainless steel, (c) schematic of lollipop specimen, and (d) photograph of the corrosion cell.*

EEC, which is discussed later. Then, the resistance offered by the steel/coating interface ($R_{P,\ S\text{-}C}$) with respect to the exposure time was monitored. A statistical approach similar to that presented in Kamde and Pillai,[14] was used for detecting the initiation of corrosion. In addition to the monitoring of $R_{P,\ S\text{-}C}$, the phase angles at low frequency (0.1 Hz) were extracted from Bode Phase plots and monitored for the specimens with FBE-coated steel rebars. Note that this phase angle is the actual impedance phase angle as measured by the EIS analyzer.

RESULTS AND DISCUSSION

3.1 | Phase 1: Field Assessment (Using Half-Cell Potential) of Fusion-Bonded-Epoxy-Coated Rebars

3.1.1 | Condition Assessment of Niles Channel Bridge

Figure 4 shows the HCP measurement at Niles Channel Bridge obtained using (i) a second reference electrode placed at one corner as a reference point (see Figure 4[a]), and (ii) the potential differential method[46] (see Figure 4[b]). The equipotential plot shows a clear potential gradient with high potential differences in the direction toward the upper center of the strut. The potential gradient plot has high gradient values in the same spot, but the area with a high probability of corrosion is restricted to a small region (between 0.9 m to 1.15 m width and 0.4 m to 0.8 m length). Unfortunately, the strut could not be autopsied for the visual inspection of FBE-coated rebars. However, as almost all of the columns and strut of this bridge have undergone corrosion and associated repairs, it can be expected that the investigated strut also has a high probability of corrosion. The potential gradients are formed either due to the corrosion of steels at locations with large coating defects and/or due to the disbondment of coating from the base metal. Generally, under this exposure condition and concrete with a chloride diffusion coefficient of $< 2 \times 10^{-11}$ m^2/s, the formation of macrocells is likely when the coating is damaged or disbonded. Consequently, it is expected that the corrosion in FBE-coated steel rebars can be detected if the defect size and corroding area in the FBE-coated steel rebar are much larger than the permitted defect sizes.

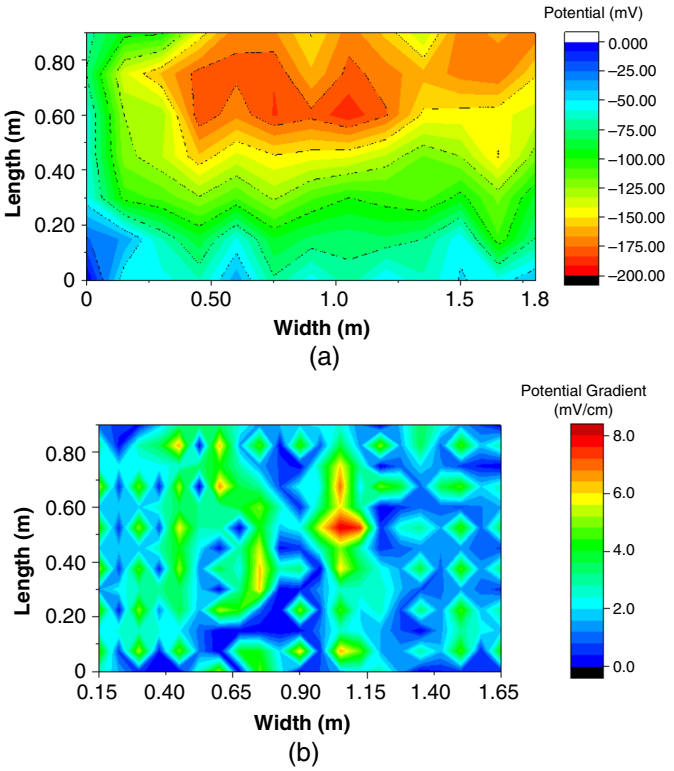

FIGURE 4. *HCP measurements and gradient plots from a strut (0.9 m × 1.8 m) of the Niles Channel Bridge. (a) Equipotential plot and (b) potential gradient plot.*

3.1.2 | Applicability of Half-Cell Potential for Corrosion Assessment of Reinforced Concrete Systems with Fusion-Bonded-Epoxy-Coated Rebars

The ability of the HCP technique in detecting corrosion in RC systems with FBE-coated rebars is significantly impaired due to the high electrical resistance of the coating. Even though the defects in the coating in the size of the permitted defect sizes can act as anodes and cathodes, no pronounced potential gradients at the concrete surface were found independent of the HCP measurement procedure. The resulting potential field in the FBE-coated rebar is dominated mainly by the resting potentials of each rebar and the moisture distribution. In the field measurements, the potential gradients up to 200 mV were measured on the concrete surface for the structure with FBE-coated rebars. It could be concluded that corrosion in FBE-coated rebars can be detected if the defect size, anode size, etc. are above some limits. The detectable anode size is probably significantly greater than the permitted defect size and the detectable anode area in conventional uncoated reinforcement. Consequently, corrosion at locations with small defects cannot be detected with HCP measurement. The rebar corrosion is detectable only after the corrosion propagates and the anode size increases significantly due to anodic or cathodic disbondment or loss of steel-coating adhesion prior to placement of concrete.

3.2 | Phase 2: Laboratory Assessment (Using Half-Cell Potential, Linear Polarization Resistance, and Electrochemical Impedance Spectroscopy) of Fusion-Bonded-Epoxy-Coated Rebars

3.2.1 | Experimental Study on the Applicability of Half-Cell Potential Measurements on Fusion-Bonded-Epoxy-Coated Rebars

The first step was the determination of the cell constant based on the geometry of the defects of the coated bar because the defect areas are the only parts of the steel surface that contribute to the electrochemical system. The resulting cell constant of the column is 3.85 cm^{-1}. The knowledge about the cell constant enables the calculation of the concrete resistivity from the concrete resistance values.[16] The concrete resistivity of both columns during the measurements was in the range of 100 Ω·m to 150 Ω·m, which is in accordance with RC systems exposed to cyclic wetting with chloride and subsequent drying.[53] In this range, reinforcement corrosion can easily be initiated and maintained.[54] Due to the relatively small sample size, the measurement grid size was chosen to be 5 cm × 5 cm.

3.2.1.1 | Influence of Half-Cell Potential Measurement Procedure

Figure 5 shows the comparison of the capability of various methods in detecting corrosion conditions of RC systems with FBE-coated steel rebars with and without short-circuit (sc) of the rebar. Figure 5(a) shows that the potential values derived from the measurement methods "ER" and "RA or RF" are close

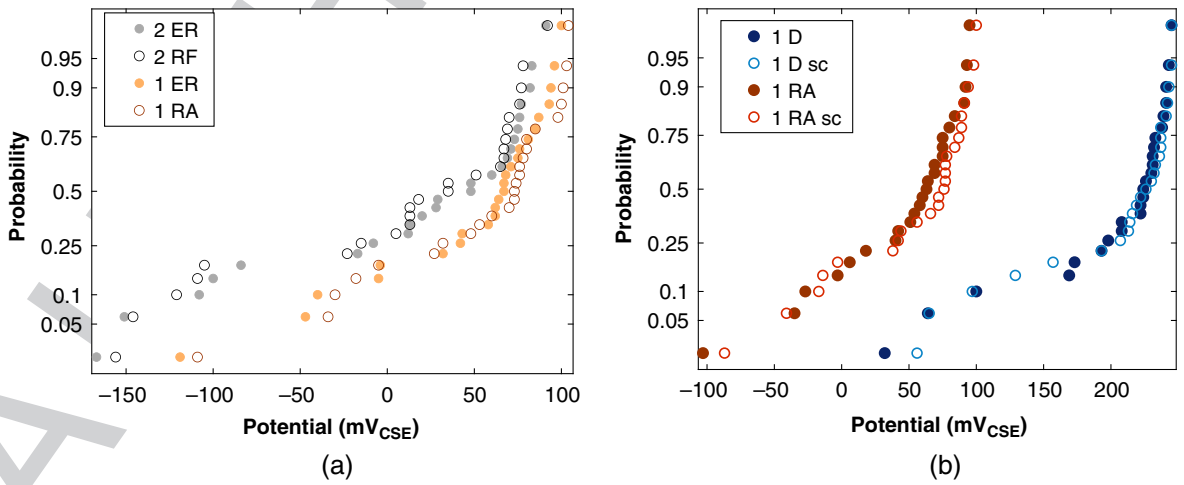

FIGURE 5. *Comparison of the three HCP measurement procedures under the two conditions: (i) no corrosion and (ii) partly short-circuited (sc); ["1" and "2"in legend indicate specimen numbers in each case]. (a) "RA or RF" and "ER" of both specimens and (b) "RA" and "D" of Specimen 1.*

to each other. The scatter between both measurement methods is in the range of typical scatter of repeated HCP measurements due to changes in the surface moisture condition.[27] The potentials of both, Specimens 1 and 2, are in a comparable range between −0.15 V_{CSE} up and 0.1 V_{CSE}—indicating no signs of rebar corrosion, which is the true corrosion condition of rebar embedded in concrete. Figure 5(b) shows the comparison of HCP measured using the procedure "D" and "RA" with open and short-circuit of the rebars. The potential readings of the differential method "D" are in a different range, but the trend of the curve and the absolute potential gradient of around 0.2 V is in good agreement with the data from the other measurement methods, "ER" and "RA" or "RF" (see Figure 5[a]). Additionally, the potential values are similar in the opened and short-circuit of the rebars—indicating that there is no difference between the methods under corrosion-free conditions. The question arises if these measurement methods will be able to detect the corrosion conditions or not, which is discussed next.

3.2.1.2 | Influence of Corrosion Condition

Figure 6 shows the probability plot of the HCPs under polarized and nonpolarized conditions measured with each measurement procedure. As expected, the intact coating with resistance greater than 5.6 MΩ prevented the electrical connectivity between rebars. When considering the HCP measurements from procedures "RA" and "D", no significant difference in the potential readings is noted when the rebars are not directly short-circuited. However, the measurement procedure "ER" indicates an increase in potential gradient due to polarization. In this case, the voltmeter is directly connected to the corroding rebar, which is normally unknown under realistic conditions. When the rebars are short-circuited to each other (i.e., electrically connected to each other) like in the case of uncoated rebars, the polarization provokes a clear shift of the potential reading, and the gradient of potential becomes more pronounced. In this case, rebar corrosion is detectable, but this situation does not represent the situation of FBE coated rebars in concrete. Therefore, it can be concluded that the corrosion of FBE-coated rebars cannot be detected using conventional HCP measurements and differential HCP measurement methods. The results from the field study presented in this paper also indicated that HCP measurements could not detect the corrosion of FBE coated rebars embedded in concrete.

3.2.2 | Condition Assessment of Fusion-Bonded-Epoxy-Coated Steel Rebars Using Linear Polarization Resistance

Figure 7 shows the linear polarization curves obtained from lollipop specimens with (a) uncoated steel rebars and (b) FBE-coated steel rebars without any intentional damage (FBEC-ND). The linear polarization curves for the uncoated steel rebars intersect the zero current line throughout the exposure time (see Figure 7[a]). The slopes of curves at that point can give rates of corrosion. For the initial exposure period, the linear polarization curves obtained from the specimens with uncoated steel rebars intersect the zero-current line between the potential range of −0.05 V_{SCE} to −0.12 V_{SCE}. This indicates that the uncoated steel rebars are in the passive state. After a few wet-dry cycles, the polarization curves started intersecting the zero-current lines between the potential range of −0.5 V_{SCE} to −0.55 V_{SCE}. This indicates the possible initiation of corrosion of uncoated steel rebars, which was later confirmed by visual

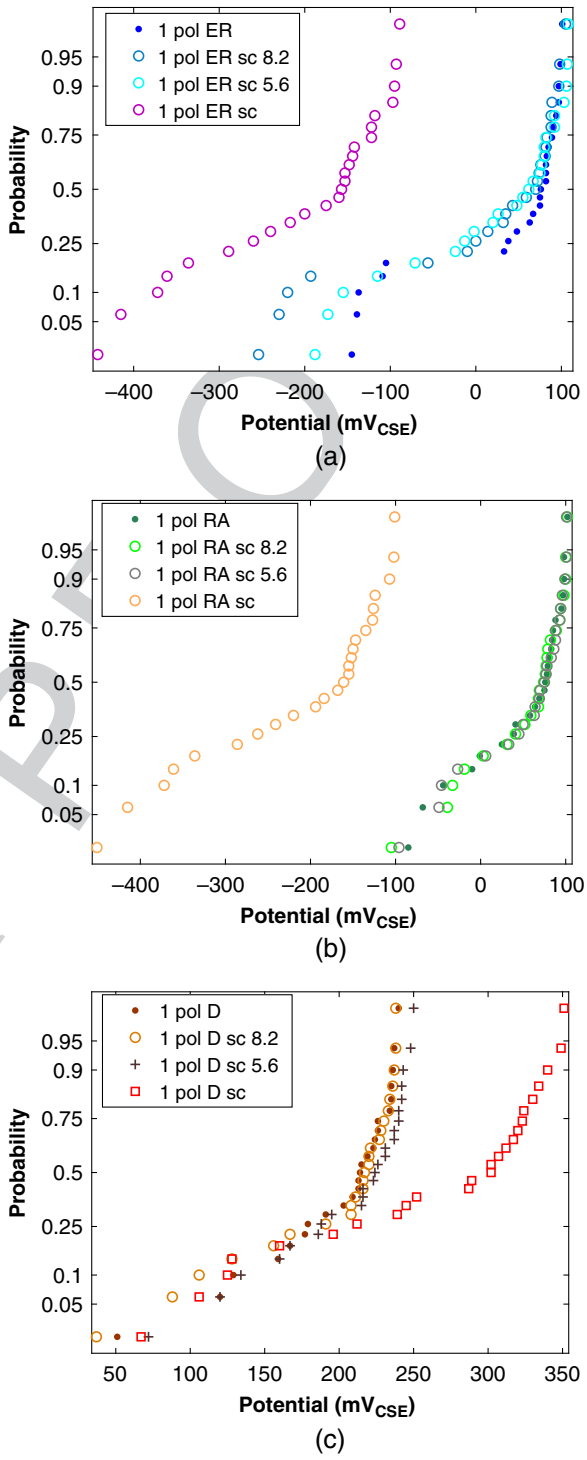

FIGURE 6. *Condition assessment of RC systems with FBE-coated steel rebar condition: polarized and partly short-circuited (sc) with different resistances in series. (a) Comparison of the HCP measurement procedures: "ER" method, (b) comparison of the HCP measurement procedures: "RF/RA" method,and (c) "D" of Specimen 1.*

inspection of corroded steel rebars extracted from lollipop specimens. Also, note that the range of values in the ordinates of the LPR curves for uncoated rebars at the initial exposure time is significantly lesser than when corrosion is initiated—which is supporting the interpretation from the measured OCPs. This

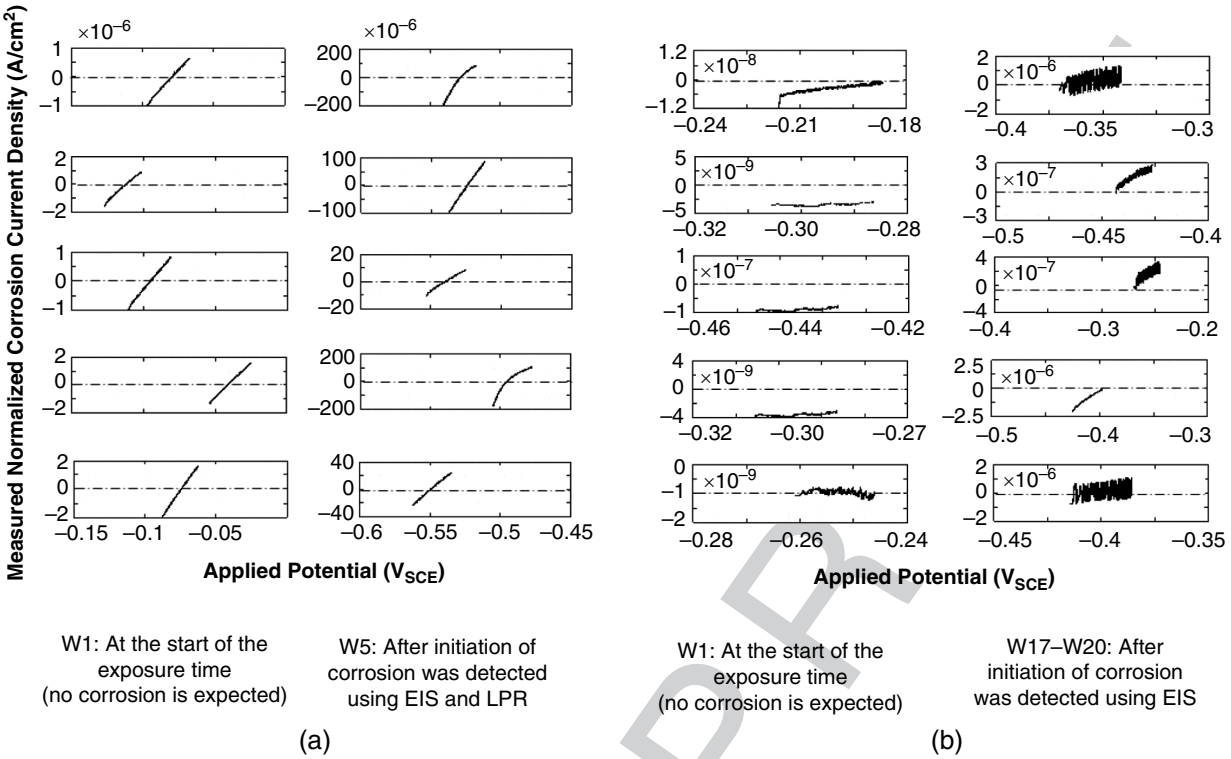

FIGURE 7. *LPR curves obtained from lollipop specimens. (Note: current density is calculated based on the total nominal surface area of rebar, equal to that of exposed steel on uncoated bars, and of coating plus coating defects on FBE coated steel rebars.)*

AQ2

indicates that the corrosion conditions of uncoated steel rebars embedded in low resistive cementitious systems can be estimated by periodic, repeated measurements of OCP or the rate of corrosion calculated using LPR data.

For specimens with FBE coated steel rebars, the linear polarization curves do not intersect the zero-current lines (Figure 7[b]). The sweep of applied potential is either in the anodic or cathodic side. Therefore, the calculation of surface-normalized resistance to polarization (R_p) using these curves was not possible. Figure 7(b) includes the response from the lollipop specimens with FBE-coated steel rebars without any intentional damage to the coating. However, the FBE coating gets damaged or degraded due to inadequate construction site practices. Such damage can result in an unintentional short-circuit of coated rebars or low electrical resistance at damaged locations of FBE coating. Specimens with such conditions may not result in such inspectability issues when tested using test methods based on LPR techniques. However, knowing locations with damage/degradation may not always be possible. Such a response can be due to the difficulties in the calculations arising from the following: (i) exact defect area of the coating or the polarized area of the steel is not known; (ii) inability of the potentiostat in measuring the OCP of steel beneath the FBE coating due to high resistance of FBE coating; and (iii) predominant reactions at steel surface is either anodic or cathodic due to localized anodic sites.[55] The sweep of ±0.015 V during polarization across the measured OCP of steel rebar did not polarize the embedded steel across the true OCP. As a result, R_P cannot be evaluated using the LPR technique for RC systems with highly resistive FBE-coated steel rebars. Also, the locations and areas of flaws such as cracks and pinholes on the FBE-coated rebars embedded in concrete structures would not be known at the time of inspection.

3.2.3 | Condition Assessment of Fusion-Bonded-Epoxy-Coated Steel Rebars Using Electrochemical Impedance Spectroscopy

Figures 8(a) and (b) show the ideal Nyquist plot from FBEC-ND steel rebars embedded in cementitious systems and the EEC, respectively. The EIS technique can capture responses from each element (i.e., cover mortar, coating, and steel/coating interface) of the working electrode or test specimen. Typical EIS response from FBE-coated steel embedded in mortar can have three pure loops corresponding to mortar, FBE coating, and steel/coating interface. The EEC from[4,28,40,56] can be modified and used to analyze the response from RC systems with FBE-coated steel rebars. The $R_{P,\ S\text{-}C}$ was quantified using the EEC. The higher the $R_{P,\ S\text{-}C}$, the lesser the corrosion rate, enabling the use of $R_{P,\ S\text{-}C}$ as one of the representative parameters to detect corrosion initiation.[57] The possibility of inspectability of RC systems with FBE-coated steel rebar using EIS is presented next.

Figures 9(a) and (b) show the typical impedance spectra (Nyquist and Bode plots) from FBEC-ND and FBEC-SD specimens, respectively. For FBEC-ND, Figure 9(a) shows that the $R_{P,\ S\text{-}C}$ at the end of the first wet period (W1) is more than 10^6 kΩ·cm^2, which is significantly high and indicates a passive state of steel rebars. At the same time, for lower frequencies (1 Hz to 0.01 Hz), the impedance is inversely proportional to the frequency (see Bode plot)—indicating that the electrochemical processes are dependent on the presence of chlorides.[34] A similar response with a slightly lower inverse relation between impedance modulus and frequency was observed after ten wet-dry exposure cycles (W10). The slow rate of change in the behavior of the Bode plot indicates that the diffusion through FBE coating is a slow process. However, once the corrosion initiates (here, at the end of about 17 to 20 wet-dry cycles), the

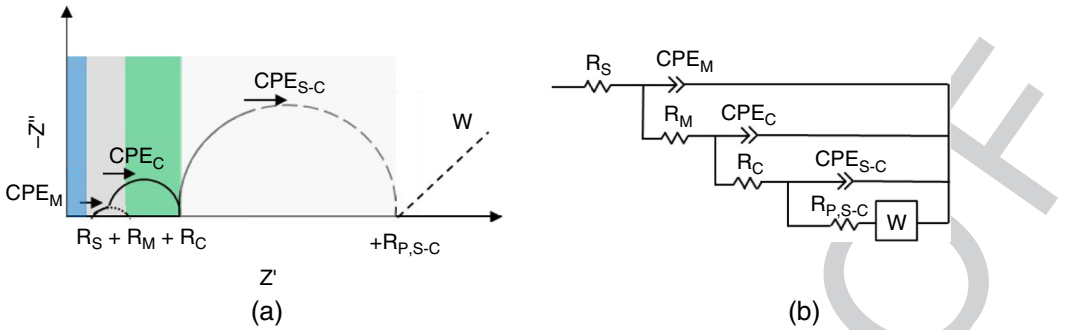

FIGURE 8. *(a) Ideal EIS response from FBE-coated steel rebar embedded in the cementitious system and (b) corresponding EEC.*[4]

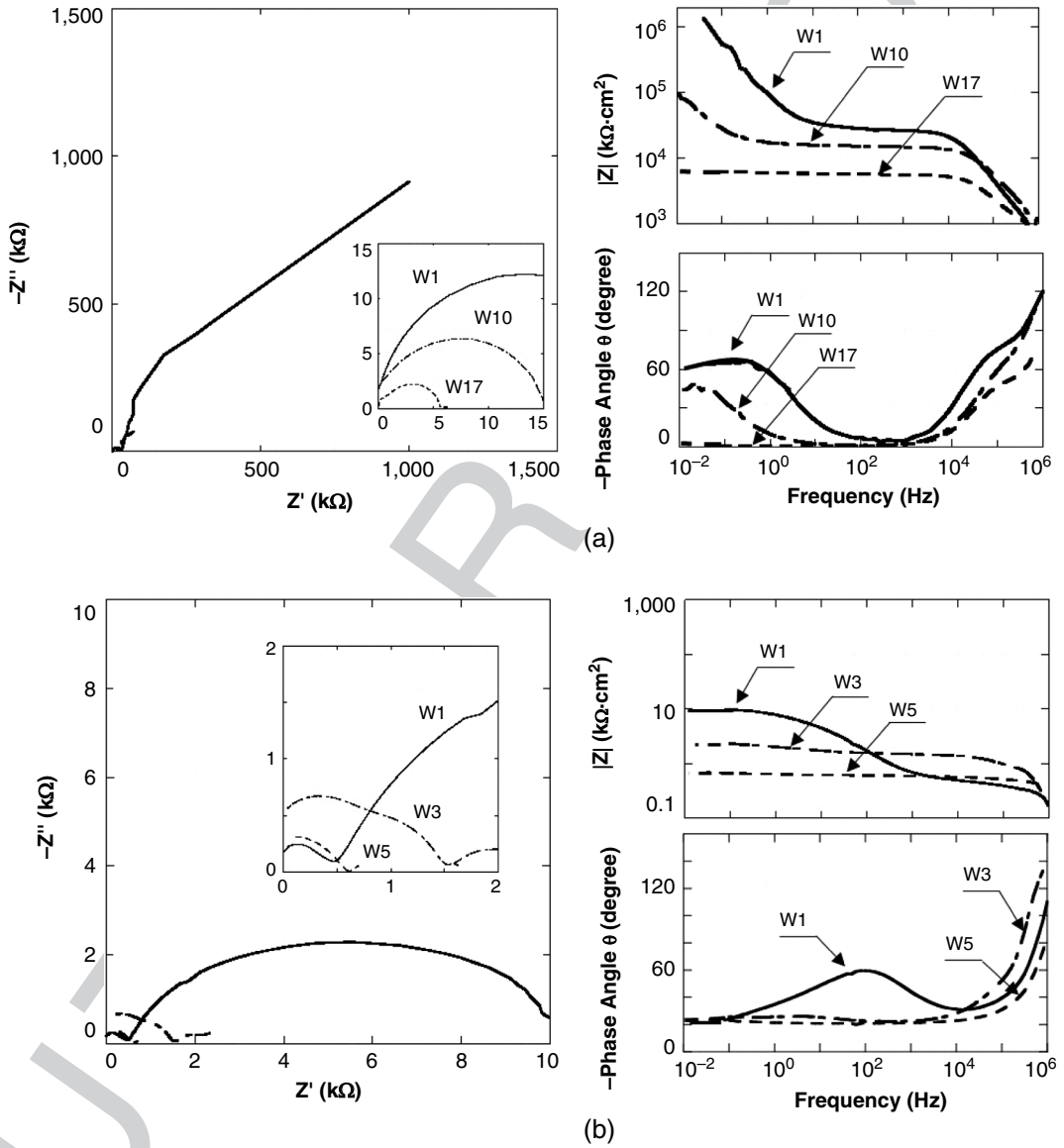

FIGURE 9. *Impedance values calculated based on total nominal rebar area at open circuit potential. (Note: W represents the number of wetting-drying cycles at the time of measurement.) (a) FBEC-ND (no damage) specimen and (b) FBEC-SD (scratch damage) specimen.*

magnitudes of impedance (denoted as |Z|) at low frequencies do not change significantly, indicating that the corrosion process is independent of further diffusion of chlorides. Therefore, after this stage, if the oxygen and moisture are available, underfilm or crevice corrosion of steel can continue without further diffusion of chlorides through the coating.

Figure 9(b) for FBEC-SD specimens shows that the magnitudes of impedance at low frequencies are constant from

the beginning of the exposure (i.e., at the end of first wet cycle W1)—indicating that the underfilm or crevice corrosion can initiate even without chlorides at steel surfaces. With further exposure to chlorides, the impedance modulus was found to be rapidly decreasing within 3 to 5 wet-dry exposure cycles (W3 to W5) using chloride solution. The decrease in the impedance modulus indicates a rapid increase in the rate of corrosion. The results presented in this paper are from laboratory-scale small specimens. The use of EIS in the field can be challenging because it is time-consuming, expensive, and difficult to conduct tests in the field due to possible heavy traffic, lack of saturation of concrete, and difficulty in accessing the structural elements with instruments. In addition, interpretation of data obtained from EIS needs expertise. Considering these challenges, use of EIS for the assessment of concrete structures with FBE-coated steel rebars is still in a nascent stage. To simplify the interpretation, this paper suggests using phase angle at low frequency to qualitatively assess the corrosion condition of steel rebar underneath the coating embedded in concrete.

Figure 10 shows the variation of phase angle (denoted as θ) at 0.1 Hz with respect to the exposure time of specimens and it is seen that the phase angle of RC systems with FBE-coated steel rebars reduces significantly at the time to initiation. For all of the specimens tested, a significant reduction in the phase angle indicated that the change in the magnitude of phase angle could give qualitative information on the corrosion of FBE-coated steel rebars. The corrosion of FBE-coated steel rebar was confirmed by visual examination of the extracted FBE-coated steel from lollipop specimens. The coating surface on extracted FBE coated steel rebars was apparently intact. However, when FBE-coated steel rebars were cut transverse or coating was peeled, the steel was corroded. The cross-sectional loss or mass loss was not carried out, as the corrosion was not significant—this stage could be identified as the initiation of corrosion. The threshold phase angle needs to be decided by testing many specimens, which is not included in the scope of this paper. Also, Figure 9(b) shows that the phase angle for FBEC-SD was found to be significantly low because the beginning of the exposure of these specimens. Therefore, the measurement of phase angle at low frequencies (e.g., frequency ≤ 0.1 Hz) can be a good representation of the corrosion condition of FBE-coated steel rebars in concrete structures. Although the phase angle does not give quantitative information, such as the rate of corrosion, it can indicate the corrosion condition of the steel underneath the coating or at locations with damaged/degraded coating. After detecting the initiation of corrosion using this approach, the lollipop specimens were autopsied, and corrosion products were observed on the steel surface. Hence, this approach based on EIS can be suitable for detecting early corrosion of FBE coated rebars in concrete.

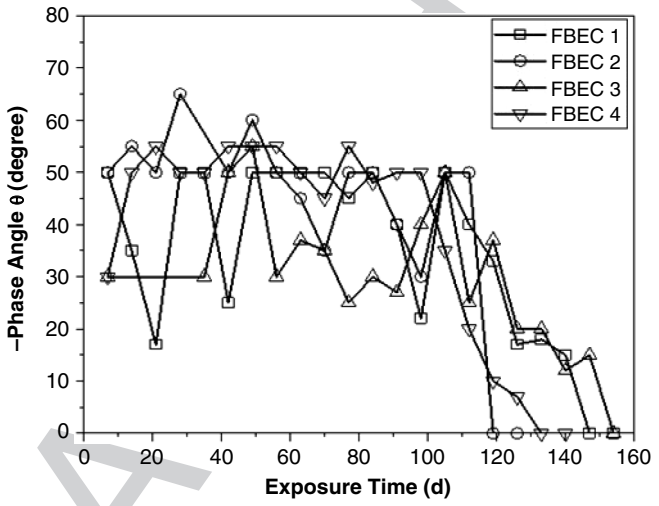

FIGURE 10. *Variation of phase angle over time with cyclic exposure of 2 d wetting with 3.5% NaCl solution and subsequent 5 d drying to the laboratory environment.*

In summary, the results presented earlier in this paper show that the test methods based on HCP and LPR could not detect the early corrosion of FBE-coated steel rebars. Test methods based on EIS show potential in detecting early corrosion on laboratory specimens. However, their validity for FBE-coated steel systems in the field is yet to be checked. This paper proposes the use of phase angle to assess the corrosion condition of RC systems with coated steel rebars, which can be a way forward for the assessment of RC systems with FBE-coated steel rebars. Another challenge in front of practitioners is to repair such infrastructure with durability in mind. The conventional patch repair may not be durable, as the underfilm/crevice corrosion and halo effect may be possible.[1,58-59] Also, the electrochemical repair may lead to coating disbondment—resulting in accelerated corrosion and bond loss between coated steel and concrete.[60] Therefore, future research on RC systems with FBE-coated steel rebar need to focus on the following areas: (i) early detection of corrosion in the field structures and (ii) designing repair strategies to arrest further corrosion without adversely affecting the steel-coating bond and hence, the rebar-concrete bond.

SUMMARY AND CONCLUSIONS

➢ The suitability of test methods based on HCP, LPR, and EIS techniques to assess the corrosion conditions of FBE-coated steel rebars in cementitious systems was investigated. The HCP technique failed to detect early corrosion. The high resistance of the coating and random damage locations on the coating makes it challenging to assess the electrochemical potential and polarization resistance of the steel underneath the FBE coating. The potential difference gradient analysis could provide information on the area with maximum corrosion probability only after the rebars undergo significant corrosion or coating disbondment. These conclusions were supplemented by results from the field and laboratory studies. Also, the assessment using LPR could not provide information on resistance to polarization due to the high resistance of the FBE coating and the unknown surface area of the exposed steel rebar. As there are no suitable techniques to quantify the defects in the coating of FBE-coated steel rebar embedded in concrete, LPR cannot be used for field assessment. On the other hand, test methods based on EIS could provide information on the resistance offered by each element of the steel-coating-concrete (S-C-C) system. It is concluded that the change in the magnitude of phase angle (at <0.1 Hz) in the EIS response can provide possible qualitative information of the ongoing corrosion activities at the steel surface embedded in mortar in laboratory specimens—and can detect corrosion initiation of FBE coated rebars in concrete. The application of the proposed EIS-based test method for field structures (with varying properties of concrete cover and coating) is yet to be validated. Also, due to the lack of adequate test methods, future research on RC systems with FBE-coated steel rebar needs to focus on detecting early

corrosion in the field structures and developing durable repair strategies without adversely affecting the rebar-concrete bond properties.

ACKNOWLEDGMENTS

The authors acknowledge the financial support (Project No. EMR/2016/003196) received from the Science and Engineering Research Board, Department of Science and Technology of Government of India. The authors also acknowledge support from the Florida Department of Transportation for granting permission to evaluate the performance of FBE-coated steel rebars in the Niles Channel Bridge and for the help accessing the bridge. The authors acknowledge the facilities in the Department of Civil Engineering at Indian Institute of Technology Madras, Chennai, India, and the Department of Civil and Environmental Engineering at the University of South Florida, Tampa, Florida, USA for conducting the laboratory experiments. The authors acknowledge the support of Professor Alberto Sagues for scientific guidance at various stages of this work.

References

1. A.A. Sagüés, K. Lau, R.G. Powers, R.J. Kessler, *Corrosion* 66 (2010): p. 065001-13.
2. F. Pianca, H. Schell, G. Cautillo, *Int. J. Mater. Prod. Technol.* 23 (2005): p. 286-308.
3. D.K. Kamde, R.G. Pillai, *Constr. Build. Mater.* 277 (2021): p. 122314.
4. D. Kamde, "Electrochemical, Bond, and Service Life Parameters of Coated Steel: Cementitious Systems Exposed to Chlorides" (Ph.D. Thesis diss., Indian Institute of Technology Madras, 2020).
5. D. Joseline, D. Kamde, S. Rengaraju, R.G. Pillai, *Sixth Int. Conf. Durab. Concr. Struct.* (2018): p. 800-806.
6. S. Kessler, J. Fischer, D. Straub, C. Gehlen, *Cem. Concr. Compos.* 47 (2014): p. 47-52.
7. S.M.S.M.K. Samarakoon, J. Sælensminde, *Cem. Concr. Compos.* 60 (2015): p. 92-98.
8. J.A. Gonzalez, M. Benito, S. Feliu, P. Rodriguez, C. Andrade, *Corrosion* 51 (1995): p. 145-152.
9. C. Andrade, C. Alonso, J. Gulikers, R. Polder, R. Cigna, Ø. Vennesland, M. Salta, A. Raharinaivo, B. Elsener, *Mater. Struct. Constr.* 37 (2004): p. 623-643.
10. C. Andrade, C. Alonso, *Constr. Build. Mater.* 10 (1996): p. 315-328.
11. D.D.N. Singh, R. Ghosh, *Corrosion* 61 (2005): p. 815-829.
12. S. Kessler, U. Angst, M. Zintel, B. Elsener, C. Gehlen, *Mater. Corros.* 67 (2016): p. 631-638.
13. X.H. Wang, Y. Gao, *Constr. Build. Mater.* 119 (2016): p. 185-205.
14. D.K. Kamde, R.G. Pillai, *Corrosion* 76 (2020): p. 843-860.
15. D.K. Kamde, M. Zintel, S. Kessler, G.P. Radhakrishna, *J. Sustain. Resilient Infrastruct.* (2021).
16. S. Kessler, M. Zintel, C. Gehlen, *Struct. Concr.* (2015): p. 398-405.
17. D.K. Kamde, R.G. Pillai, "Comparison of Corrosion of Damaged Fusion-Bonded-Epoxy-Coated (FBEC) and Uncoated Steel Rebars," in Int. Conf. Adv. Constr. Mater. Syst. (Chennai, India: RILEM, 2017).
18. S. Kessler, K. Lau, A.A. Sagüés, "Extent of Cathodic Reaction on Epoxy-Coated Rebar with Partially Disbonded Coating," CORROSION 2017 (Houston, TX: NACE International, 2017), p. 1-12.
19. A.A. Sagues, R.G. Powers, R. Kessler, "Corrosion Performance of Epoxy-Coated Rebar in Florida Keys Bridges," CORROSION 2001 (Houston, TX: NACE, 2001).
20. S. Rengaraju, A. Godara, P. Alapati, R.G. Pillai, *Mag. Concr. Res.* 72 (2020): p. 194-206.
21. ASTM C876, (West Conshohocken, PA: ASTM International, 2015).
22. B. Elsener, C. Andrade, J. Gulikers, R. Polder, M. Raupach, *Mater. Struct. Constr.* 36 (2003): p. 461-471.
23. SIA Merkblatt, "Planung, Durchführung Und Interpretation Der Potentialfeldmessung an Stahlbetonbaute," *Schweizerischer Ingenieur- und Architekten-Verein* (Berlin, Germany: German Society for Non-Destructive Testing (DGZfP), 2006).
24. DGZfP Specification B3, "Electrochemical Half-Cell Potential Measurements for the Detection of Reinforcement Corrosion" (Berlin, Germany: German Society for Non-Destructive Testing, 2014).
25. M.F. Montemor, A.M.P. SimÃµes, M.M. Salta, *Cem. Concr. Compos.* 22 (2000): p. 175-185.
26. S. Keßler, C. Gehlen, *J. Infrastruct. Syst.* 23 (2017).
27. S. Keßler, C. Gehlen, *Beton- Und Stahlbetonbau* 108 (2013).
28. K. Lau, A.A. Sagüés, *Electrochem. Soc.* 3 (2007): p. 81-92.
29. S. Keßler, A.A. Sagüés, *Mater. Corrosion* 71 (2020): p. 849-856.
30. J.A. Pincheira, A. Aramayo, D. Fratta, K.-S. Kim, *J. Perform. Constr. Facil.* 29 (2015): article 04014097.
31. B. Goffin, "Non-Destructive Detection of Corrosion of Epoxy Coated Rebars" (Ph.D. Thesis diss., Department of Civil Engineering, The University of British Columbia, Vancouver, 2017).
32. O.S.B. Al-Amoudi, M. Maslehuddin, M. Ibrahim, *ACI Mater. J.* 101 (2004): p. 303-309.
33. J.W. Wu, D. Bai, A.P. Baker, Z.H. Li, X.B. Liu, *Mater. Corros.* 66 (2015): p. 143-151.
34. A.A. Sagüés, A.M. Zayed, *Corrosion* 47 (1991): p. 852-859.
35. K. Lau, "Corrosion Performance of Concrete Cylinder Piles" (Ph.D. Thesis diss., Department of Civil and Environmental Engineering, University of South Florida Major, 2006).
36. A. Cao-Paz, A. Covelo, J. Farina, X. R. Nóvoa, C. Pérez, L. Rodríguez-Pardo, *Prog. Org. Coat.* 69 (2010): p. 150-157.
37. A. Miszczyk, K. Darowicki, *Prog. Org. Coat.* 124 (2018): p. 296-302.
38. F. Tang, G. Chen, R.K. Brow, M.L. Koenigstein, "Electrochemical Characteristics and Equivalent Circuit Representation of Mortar-Coating-Steel Systems by EIS," CORROSION 2014 (Houston, TX: NACE, 2014), p. 1-10.
39. L. Xing, D. Darwin, J. Browning, "Evaluation of Multiple Corrosion Protection Systems and Corrosion Inhibitors for Reinforced Concrete Bridge Decks" (Lawrence, Kansas, 2010).
40. A.A. Sagues, *Corrosion* 44 (1988): p. 555-557.
41. A.A. Sagues, R.G. Powers, "Effect of Concrete Environment on the Corrosion Performance of Epoxy-Coated Reinforcing Steel," CORROSION 1990 (Houston, TX: NACE, 1990).
42. S. Rengaraju, R.G. Pillai, *Constr. Build. Mater.* 305 (2021).
43. K. Lau, A. Sagüés, *Electrochim. Acta* 56 (2011): p. 7815-7824.
44. H.H. Hernández, A.M.R. Reynoso, J.C.T. González, C.O.G. Morán, J.G.M. Hernández, A.M. Ruiz, J.M. Hernández, R.O. Cruz, "Electrochemical Impedance Spectroscopy (EIS): A Review Study of Basic Aspects of the Corrosion Mechanism Applied to Steels," in *Electrochem. Impedance Spectrosc.* (IntechOpen, 2013), p. 137-144.
45. ASTM A775, "Standard Specification for Epoxy-Coated Steel Reinforcing Bars" (West Conshohocken, PA: ASTM International, 1981).
46. K. Reichling, M. Raupach, *Bautechnik* 90 (2013): p. 715-720.
47. K. Lau, A.A. Sagüés, *Corrosion* 65 (2009): p. 681-694.
48. M. Zintel, U. Angst, S. Keßler, C. Gehlen, *Beton- Und Stahlbetonbau* 109 (2014).
49. ASTM A775, "Standard Specification for Epoxy-Coated Steel Reinforcing Bars 1" (West Conshohocken, PA: ASTM International, 2017).
50. N. Elgrishi, K.J. Rountree, B.D. McCarthy, E.S. Rountree, T.T. Eisenhart, J.L. Dempsey, *J. Chem. Educ.* 95 (2018): p. 197-206.
51. S. Rengaraju, L. Neelakantan, R.G. Pillai, *Electrochim. Acta* 308 (2019): p. 131-141.
52. M.A. Ameer, E. Khamis, M. Al-Motlaq, *Corros. Sci.* 46 (2004): p. 2825-2836.
53. R.B. Polder, *Constr. Build. Mater.* 15 (2001): p. 125-131.
54. K. Hornbostel, C.K. Larsen, M. Geiker, "Relationship between Concrete Resistivity and Corrosions Rate– a Literature Review," in Proc. Int. Conf. Durab. Concr. (Trondheim, 2012).
55. B.O. Yang, "Differencial Flow through Cell Technique," in *Techniques for Corrosion Monitoring*, ed. L. Yang, (Woodhead Publishing Series, 2008).
56. X.H. Wang, B. Chen, Y. Gao, J. Wang, L. Gao, *Constr. Build. Mater.* 93 (2015): p. 746-765.
57. C. Andrade, *Indian Concr. J.* 94 (2020): p. 1-9.
58. M. Raupach, *Cem. Concr. Compos.* 28 (2006): p. 679-684.
59. K. Lau, A.A. Sagüés, R.G. Powers, *Corrosion* 66 (2010): p. 0650021-06500216.
60. D.K. Kamde, R.G. Pillai, "Effect of the Degree of Corrosion on Bond Performance of Cement Polymer Composite (CPC) Coated Steel Rebars," in Int. Conf. Concr. Repair, Rehabil. Retrofit. (2018), p. 3-7.

AQ3 AQ4 AQ5 AQ6 AQ7 AQ8 AQ9

Queries

AQ1: Please provide post code for affiliations *,**,***.
AQ2: Please provide part label description in caption of Figure 7.
AQ3: Please provide volume number for References 5,16.
AQ4: Please provide volume and page range for Reference 15.
AQ5: Please provide title for Reference 21.
AQ6: Please provide page range for References 26, 27,42.
AQ7: Please provide publisher name for References 39,54.
AQ8: Please check and provide complete book title, and also provide publisher location for References 44,55.
AQ9: Please provide publisher name and location for Reference 60.